A Novel Secondary DNA Binding Site in Human Topoisomerase I Unravelled by using a 2D DNA Origami Platform

Ramesh Subramani,[†,#] Sissel Juul,[‡,#] Alexandru Rotaru,[†,§] Felicie F. Andersen,[‡] Kurt V. Gothelf,[†,§] Wael Mamdouh,[†,⊥] Flemming Besenbacher,[†,∥] Mingdong Dong,[†,*] and Birgitta R. Knudsen[‡,*]

[†]Interdisciplinary Nanoscience Center (iNANO), Centre for DNA Nanotechnology (CDNA), [‡]Department of Molecular Biology, [§]Department of Chemistry, and [∥]Department of Physics and Astronomy, University of Aarhus, Nordre Ringgade 1, DK-8000 Aarhus C, Denmark. [⊥]Current address: Department of Chemistry, School of Sciences and Engineering, The American University in Cairo (AUC), Egypt. [#]These authors contributed equally to this work.

ABSTRACT The biologically and clinically important nuclear enzyme human topoisomerase I relaxes both positively and negatively supercoiled DNA and binds consequently DNA with supercoils of positive or negative sign with a strong preference over relaxed DNA. One scheme to explain this preference relies on the existence of a secondary DNA binding site in the enzyme facilitating binding to DNA nodes characteristic for plectonemic DNA. Here we demonstrate the ability of human topoisomerase I to induce formation of DNA synapses at protein containing nodes or filaments using atomic force microscopy imaging. By means of a two-dimensional (2D) DNA origami platform, we monitor the interactions between a single human topoisomerase I covalently bound to one DNA fragment and a second DNA fragment protruding from the DNA origami. This novel single molecule origami-based detection scheme provides direct evidence for the existence of a secondary DNA interaction site in human topoisomerase I and lends further credence to the theory of two distinct DNA interaction sites in human topoisomerase I, possibly facilitating binding to DNA nodes characteristic for plectonemic supercoils.

KEYWORDS: atomic force microscopy (AFM) · functionalized 2D origami · human topoisomerase I · secondary binding site · supercoil recognition

Human topoisomerase I (hTopoIB) is a typical representative of the nuclear forms of the eukaryotic typeIB topoisomerases, being a monomeric enzyme of 91 kDa (765 amino acids), which relaxes topological tension in the genome by introducing transient single-stranded breaks in the DNA. This is accomplished by the enzyme using an active site tyrosine as a nucleophile to attack a phosphodiester bond in the DNA backbone generating a 3′-phosphotyrosyl linkage and leaving a 5′-hydroxyl DNA end free to rotate around the intact strand. This mechanism of action allows hTopoIB to relax both negative and positive supercoils, *i.e.*, under- and overwound DNA, respectively, before rejoining the cleaved DNA strand.[1]

Consistent with the need for hTopoIB activity at multiple genomic locations, the enzyme binds and cleaves double-stranded DNA with preference for only a very degenerate consensus sequence (5′-(T/A)(G/C/A)(T/A)(T/C/A)-3′).[2−4] Hence, instead of a base sequence, hTopoIB recognizes DNA in a topology dependent manner showing a strong preference for supercoiled DNA of both signs over relaxed forms of circular DNA.[5−10] Traditionally, hTopoIB has been envisioned as binding only one site on the DNA helix at a time (as outlined by the crystal structure of hTopoIB in covalent complex with DNA, Figure 1A (modified from ref 11). However, emerging evidence challenges this conclusion, and recently it was suggested that the existence of a secondary DNA binding domain in the enzyme allows simultaneous interaction to two DNA sites (Figure 1B, interaction mode T_1),[9,10,12−14] which may account for the preferred interaction to supercoiled DNA of either positive or negative sign. Note, that supercoiled DNA regardless of sign is characterized by a high degree of intramolecular nodes, *i.e.*, double-strand DNA crossovers. The first evidence for this theory was provided by electron microscopy (EM) demonstrating binding of nuclear TopoIB to intramolecular DNA crossovers,[9] which was suggested to facilitate DNA supercoil recognition. In later reports most evidence supporting the existence of a secondary binding site in typeIB topoisomerases has been provided from analyses of bacterially or virally expressed so-called "minimal" members of the enzyme family. These enzymes differ from nuclear TopoIB by lacking the rather extensive N-terminal and -linker domains and by showing a clear sequence preference in DNA cleavage promoted by a "specificity helix" in the enzyme.[1,15] In these aspects, the minimal TopoIBs are more

*Address correspondence to dong@inano.au.dk, brk@mb.au.dk.

Received for review July 16, 2010 and accepted August 26, 2010.

Published online September 9, 2010. 10.1021/nn101662a

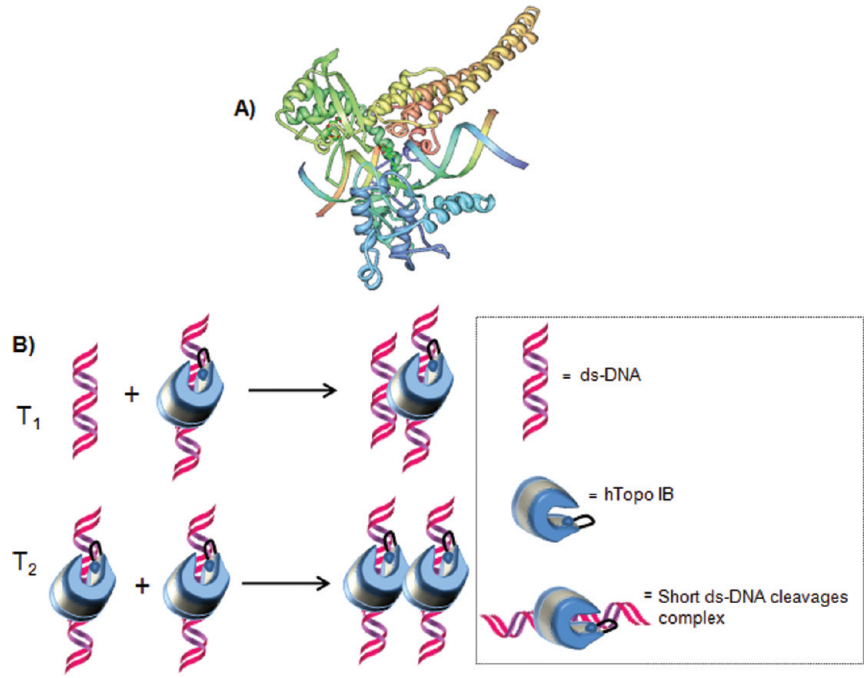

Figure 1. (A) X-ray crystallographic structure of hTopoIB in complex with DNA (modified from ref 11). The dimensions of the globular part of the enzyme (lacking the N-terminal and -linker domains) are approximately 6 × 6 × 6 nm.[29] (B) Schematic representation of putative interaction modes between TopoIB and DNA that may explain node and filament formation on relaxed circular DNA. Interaction mode T_1 is simultaneous interaction of one TopoIB to two DNA helices. Interaction mode T_2 is interaction between two TopoIB−DNA complexes.

reminiscent to the typeIB topoisomerase-related tyrosine recombinases than are the nuclear typeIB topoisomerases.[15,16]

Using the minimal TopoIB from vaccinia virus (vvTopoIB), it was demonstrated by EM[12] and atomic force microscopy (AFM) imaging[13] that this enzyme promotes formation of intra- or intermolecular synapses in which DNA segments are brought together at protein-containing nodes or within filamentous protein stems. Such synapses could be facilitated by a secondary binding site in vvTopoIB (Figure 1B, T_1 interaction mode) or via contacts between two vvTopoIB−DNA complexes, possibly promoted by direct protein−protein interactions (as outlined in Figure 1B, T_2 interaction mode). In favor of the T_2 interaction mode is the close kinship between typeIB topoisomerases and tyrosine recombinases, of which members of the latter family are well-known to promote DNA synapses via specific protein−protein interactions.[17,18] However, the recent crystallization of the minimal typeIB topoisomerase from *Deinococcus radiodurans* (draTopoIB) in complex with DNA revealed a secondary DNA binding site in this enzyme,[14] which very likely accounts for DNA cross-over binding and generation of protein-containing nodes or filamentous plectonemes at least for the bacterial and viral minimal typeIB topoisomerases.

The secondary binding site in draTopoIB is located on the surface of the C-terminal domain spanning amino acids 106−129.[14] Interestingly, a recent study identified a cluster of four lysines in hTopoIB, situated within the putative equivalent region of the draTopoIB secondary binding site, as important contributors to the preferred binding of hTopoIB to supercoiled DNA.[10] This observation suggests that a secondary DNA binding site may be a common feature of all typeIB topoisomerases, including the quite large nuclear types, possibly providing a "topological sensor" that directs the enzyme to plectonemic DNA.

However, the existence of a secondary binding site in nuclear typeIB topoisomerases has never been addressed directly. In the present study we use AFM imaging to demonstrate that, like vvTopoIB, hTopoIB also promotes formation of synapses between separate DNA segments in protein containing nodes or filaments. We address the molecular mechanism behind this synapsis formation by taking advantage of a fully programmable and addressable two-dimensional (2D) DNA origami template to investigate the interaction between single hTopoIB enzymes or enzyme−DNA complexes to other DNA segments or complexes. In the DNA origami method, a long single-stranded DNA sequence of typically 7200 nucleotides is folded by >200 short synthetic oligonucleotides into parallel aligned helices held together by crossovers.[19] During recent years, 2D rectangular DNA origamis have been used as templates to create desired surface modifications at well-defined positions with approximately 6 nm resolution.[19] This has successfully enabled programmable exposure of CNTs,[20] gold nanoparticles,[21,22] and biomolecules.[23−26] Recently, we have shown that a DNA origami can be applied as a platform for studying single molecule chemical reactions.[27] In the present

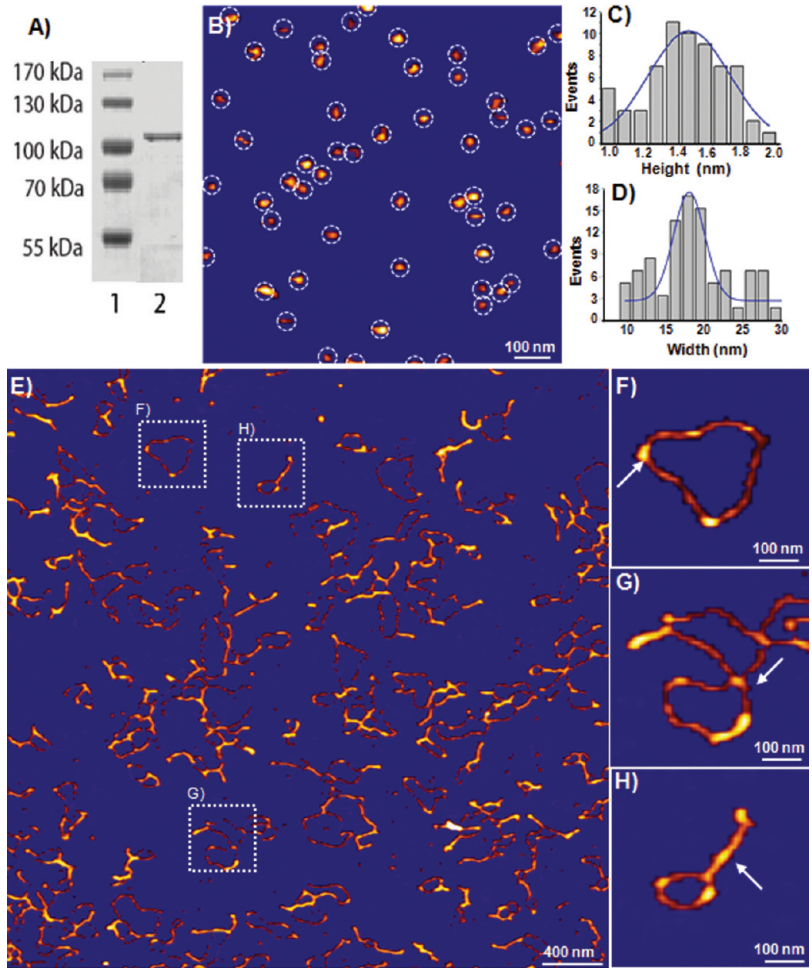

Figure 2. (A) sodium dodecyl sulfate (SDS) polyacrylamide gel electrophoretic analysis of purified hTopoIB (lane 2) run next to a protein marker (lane 1). The sizes of the marker proteins are indicated to the left of the gel picture. (B) AFM topography image of hTopoIB in a liquid environment. Each individual enzyme is marked with a white circle. (C) Height and (D) width histograms of hTopoIB measured from images like the one shown in (B) with the Gaussian fittings indicated in blue. (E) Large-scale AFM image performed in air of hTopoIB bound to relaxed circular DNA. The prevalent types of hTopoIB−DNA binding modes have been highlighted with white squares in (E) and are shown as zoom-in images in (F−H) depicting an isolated binding event, an intermolecular node, and a filament structure, respectively.

study we demonstrate the successful application of 2D DNA origami nanostructures to monitor protein−DNA interactions and reveal a simultaneous interaction of hTopoIB with two different DNA molecules. The presented results strongly advocate for the existence of a secondary DNA binding site in nuclear typeIB topoisomerases.

RESULTS AND DISCUSSION

AFM Analysis of Purified hTopoIB in Solution. Recombinant hTopoIB for the AFM study was expressed and purified as described previously.[28] The purity of the enzyme was analyzed by denaturing gel electrophoretic separation followed by Coomassie staining of the resulting gel. As evident in Figure 2A, the Coomassie staining revealed only a single protein band in purified protein fractions with a gel electrophoretic mobility of approximately 100 kDa, corresponding to the expected mobility of hTopoIB (Figure 2A, lane 2). The identity of this protein as hTopoIB was confirmed by Western blotting (data not shown).

AFM operated under liquid environment was used to determine the size of single hTopoIB molecules. As depicted in Figure 2B, the AFM images revealed a uniform distribution of asymmetrical nanostructures, adsorbed on the 2D solid surfaces with random orientation. The measured average height of hTopoIB enzymes obtained by fitting the Gaussian function to the AFM images was 1.4 ± 0.3 nm, (Figure 2C) and, hence, differed considerably from the approximate height of 6−7 nm, as determined by X-ray crystallography[29] (Figure 1A). This apparent height difference is likely to be explained by AFM tip compression and surface adsorption forces in the AFM studies, since hTopoIB in liquid most probably should be considered a rather flexible 3D object. Hence, when hTopoIB is immobilized to the negatively charged mica surface, the strong electrostatic interaction with positively charged areas of the enzyme may introduce a certain degree of deformation.

In addition, distortion from the force exerted by the AFM tip, apparently results in elongation of enzymes along the scan direction. This effect could not be avoided by adjusting AFM imaging parameters to apply a lower force. Even at these conditions the height of hTopoIB appeared to be less than 25% of the height determined by X-ray crystallography. Detailed quantitative size analyses of single enzymes along the *XY*-dimensions revealed that the hTopoIB widths ranged from 10 to 30 nm, with the average diameter of hTopoIB being estimated to 17.0 ± 3.5 nm by fitting to the Gaussian function, as shown in Figure 2D. Although AFM tip convolution is always involved when imaging objects smaller than the tip radius (in this study, the tip radius was 10 nm), the increased value of *XY*-dimensions and decreased value of the *Z*-dimension (relative to the crystal dimensions) most probably can be ascribed mainly to the molecule conformation on the 2D mica surfaces. The above results provide the reference values for detecting single hTopoIB molecules on the 2D DNA origami platform used for the further AFM studies presented here.

AFM Imaging of hTopoIB in Complex with Relaxed Circular DNA. As mentioned earlier, vvTopoIB was previously found to form filaments on circular DNA by intramolecular synapsis between two segments of a single DNA molecule.[12,13] To investigate if a similar DNA interaction pattern could be observed for the much larger human enzyme, purified hTopoIB was mixed with relaxed circular DNA in a molar ratio of 4:1 and incubated for 5 min at room temperature before AFM imaging of the resulting products. Figure 2E shows a representative example of a large-scale AFM image obtained by this analysis. Consistent with the previously published binding mode of vvTopoIB,[13] incubation of hTopoIB with circular DNA resulted in three different types of structural motifs on the surface including: (i) isolated binding, (ii) nodes, and (iii) filament-like structures (examples of the different binding modes are indicated by arrows in Figure 2F−H). The node structure revealed in Figure 2G brings two DNA circles together and, hence, clearly involves two helices from two different DNA molecules. The filament structure depicted in Figure 2H also involves two DNA helices, although from the same DNA molecule, as revealed by comparing the contour length of the filament-containing DNA circle with the contour length of a DNA circle without filaments (Figure 2F). Hence, the full contour length of the DNA molecule depicted in Figure 2H equals the contour length of the DNA molecule without filament formation (Figure 2F) only if the filament stretch contains two DNA helices.

The formation of numerous node and filament structures upon incubation of hTopoIB with relaxed circular DNA, as revealed by AFM imaging in Figure 2, strongly suggests that hTopoIB, like vvTopoIB, promotes synapsis formation between two DNA helices from either the same or different DNA molecules. However, whether such synapsis formation can be ascribed to a secondary DNA binding site in the enzyme (interaction mode T_1) or to the ability of two hTopoIB−DNA complexes to bind each other (interaction mode T_2) was not addressed by the AFM imaging shown in Figure 2.

Experimental Design for Investigation of the Putative T_1 or T_2 Interaction Modes of hTopoIB. To investigate the molecular background for the node and filament structures observed in Figure 2E, we chose a 2D rectangular 100 × 70 nm^2 DNA origami structure as a platform for studying the hTopoIB−DNA interactions at the single molecule level. The 2D DNA origami was folded from a long single-stranded M13mp18 segment and 225 synthetic oligonucleotides (staple strands). The unique aspect of the 2D origami is that the positions on the 2D array are fully addressable as previously described[19] (see Supporting Information, Figure S1). In a selected position on the DNA origami template, one of the staple strands was extended with a stretch of 21 nucleotides which was hybridized with a complementary sequence to expose a 21 base pair double-stranded DNA (baitDNA) fragment extending from the surface (Figure 3A). This allowed for the putative interaction of hTopoIB in covalent complex with DNA and, thereby, having the primary DNA interaction site occupied, to a second DNA helix (interaction mode T_1) or to another hTopoIB−DNA complex (interaction mode T_2) to be addressed. The interaction mode T_1 was addressed directly by adding purified hTopoIB−DNA cleavage complexes to the DNA origami template (Figure 3A and B) before the samples were imaged by AFM in a liquid environment. The interaction mode T_2 required a two-step measurement: In the first step, the baitDNA protruding from the origami template was bound by purified hTopoIB (Figure 3C), and in the second step, purified cleavage complexes were added to the 2D origami (Figure 3D). Subsequently, putative interactions were visualized by AFM imaging in a liquid environment.

AFM Analysis of Interaction Mode T_1 (One hTopoIB Interacting with Two DNA Helices). To address the interaction mode T_1, hTopoIB−DNA cleavage complexes were added to the DNA origami, as outlined in Figure 3A and B. First the DNA origami was assembled with the protruding baitDNA, and second the origami sample was deposited on a freshly cleaved mica surface. As expected, the AFM imaging revealed the formation of the 2D rectangular DNA origami scaffolds (Figure 4A). The protruding baitDNA was not visible in the AFM images due to the flexibility of double-stranded DNA in the aqueous phase. Purified hTopoIB−DNA cleavage complexes (see Supporting Information, Figure S2) were subsequently added to the immobilized DNA origami templates on the mica surface (as outlined in Figure 3A and B). After 30 min incubation at room temperature, excess and unspecifically bound cleavage complexes were removed by washing with a high-salt buffer (500 mM of NaCl) followed by three times washing of the

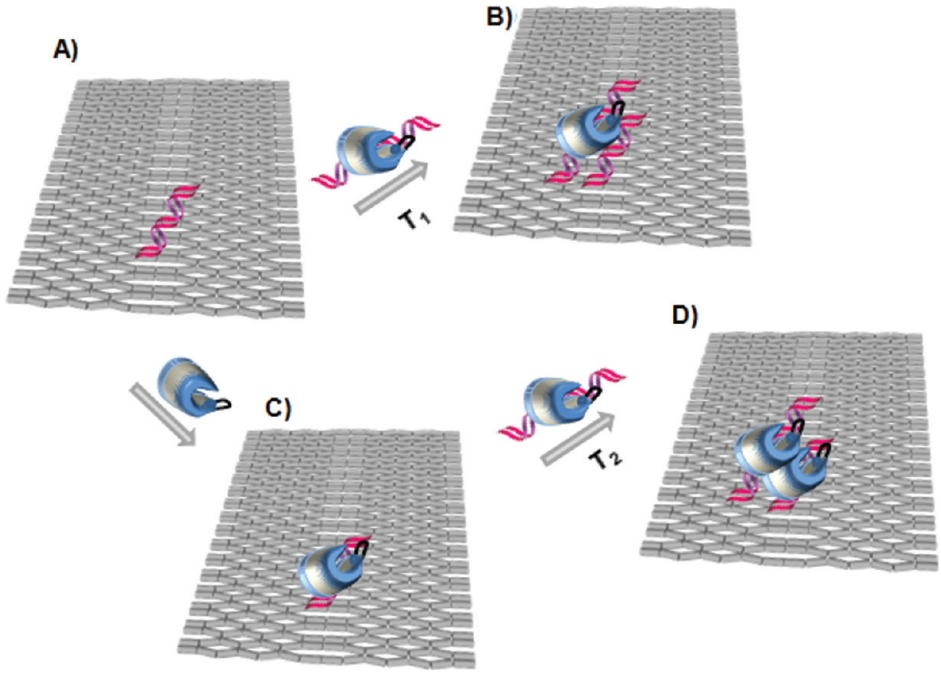

Figure 3. Schematic diagram explaining the experimental design for investigating the T_1 or T_2 interaction mode of hTopoIB. (A) Shows the double-stranded baitDNA protruding from the origami. (B) Shows the experimental setup for investigating the T_1 interaction mode of hTopoIB. The hTopoIB−DNA cleavage complexes are added to the DNA origami with the protruding baitDNA, and the interaction measured by AFM imaging in a liquid environment. (C) and (D) Show the two-step experimental setup for investigating the T_2 interaction mode of hTopoIB. In the first step, (C), free hTopoIB is bound to the baitDNA on the origami. In the second step, (D) purified cleavage complexes are added to the DNA origami before visualization by AFM in a liquid environment.

mica surface with slightly warm TAEM buffer. As shown in Figure 4B, AFM imaging clearly revealed the appearance of nanoparticles on top of several of the origami templates. These nanoparticles were identified as hTopoIB−DNA cleavage complexes, since their heights were determined to be approximately 1.5 nm by cross-section analysis of the naked and particle-bound origami surface (Figure 4E and F). This height is in a good agreement with the height analysis of hTopoIB on the mica surface (Figure 2C). Note, that in all images no more than one nanoparticle were observed on a single origami template. This observation strongly argues against unspecific binding of the hTopoIB cleavage complexes to the origami surface since, spatially, this surface of 100 × 70 nm^2 can easily support binding of numerous such complexes. This notion is further supported by the fact that binding of hTopoIB to DNA origami templates without the baitDNA does not occur (data not shown). Hence, we conclude that the observed nanoparticles can be ascribed to specific binding between the hTopoIB cleavage complexes and the baitDNA protruding from the DNA origami.

To determine quantitatively the hTopoIB−DNA cleavage complex to DNA binding efficiency, 278 2D origami tiles were arbitrarily chosen from the AFM images, and the percentage bound by hTopoIB cleavage complexes was determined to be 30.7 ± 9%. In the context of the binding percentage it is important to point out that the origamis can be faced two ways on the mica surface, *i.e.*, face-up, exposing the baitDNA, or face-down, covering the baitDNA, and hence, some of the 2D origamis are likely not to expose the baitDNA for hTopoIB binding.

AFM Analysis of Interaction Mode T_2 (Interaction between Two hTopoIB−DNA Complexes). For investigating the interaction mode T_2, the first step was to prepare DNA origamis exposing hTopoIB-bound baitDNA (Figure 3C). These were prepared by incubating purified hTopoIB with the 2D origami templates for 30 min, followed by washing with a high-salt buffer (500 mM NaCl) and warm TAEM, as described above. Subsequent AFM imaging confirmed hTopoIB binding to the baitDNA on the 2D DNA origami (Figure 4C). It should be noted that, as mentioned above, hTopoIB did not bind to the DNA origami templates without baitDNA (data not shown). From the AFM images and the determined height and width values of hTopoIB on the mica surface (Figure 2C and D), each nanoparticle on the origami templates (an example is indicated by an arrow in Figure 4C) corresponds to the binding of a single hTopoIB enzyme. The binding percentage of hTopoIB to the baitDNA was calculated by randomly choosing 285 DNA origami templates, which resulted in a yield of 28.3 ± 5%. As argued above, this yield may correspond to a higher effective binding efficiency of hTopoIB to the actually exposed baitDNA (due to the random orientation of 2D origami templates on the mica surface, *i.e.*, both face-up and -down configurations exist).

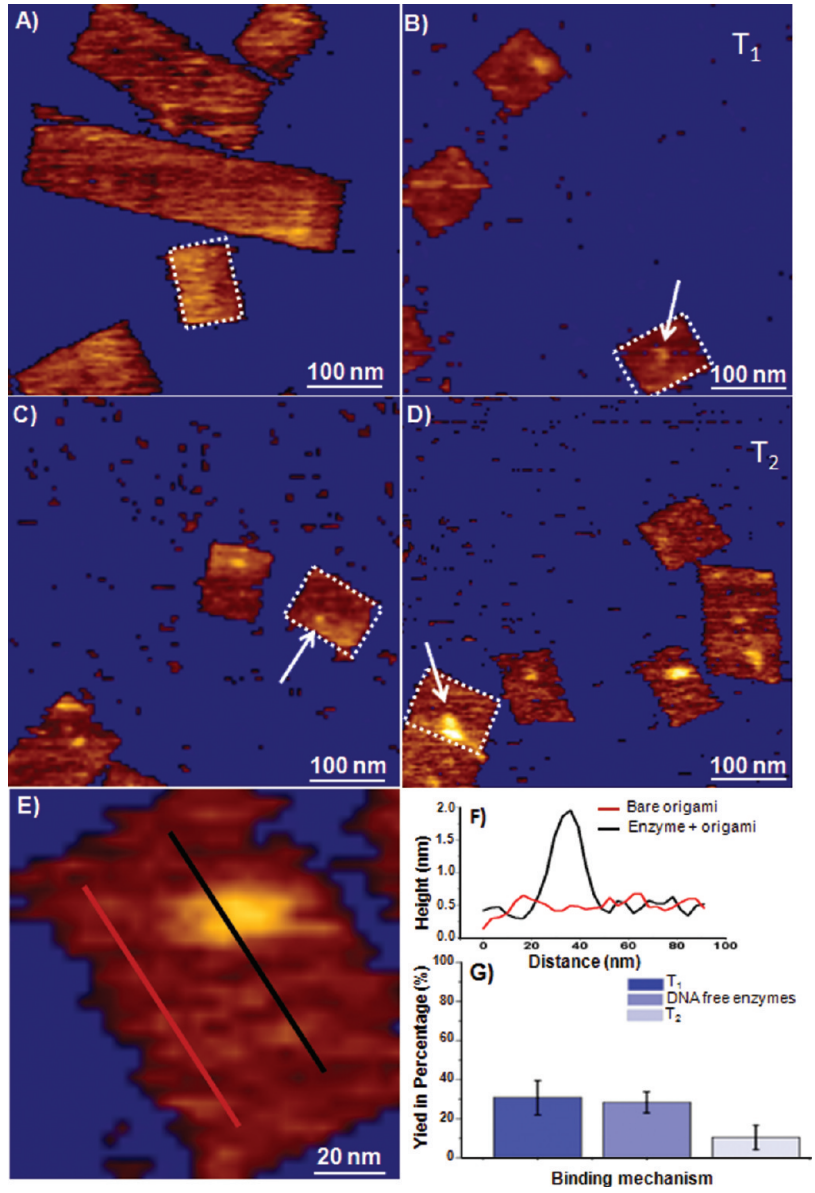

Figure 4. AFM analysis of interaction modes T_1 and T_2. (A) AFM image of rectangular DNA origami scaffolds adsorbed on the mica surface (one DNA origami has been highlighted with a white square). (B) AFM image of DNA origamis after incubation with purified hTopoIB−DNA cleavage complexes for the investigation of interaction mode T_1. One DNA origami has been highlighted with a white square, and the white arrow points to a hTopoIB−DNA cleavage complex bound to the DNA origami. (C) AFM imaging of DNA origamis after incubation with hTopoIB (the first step in the investigation of interaction mode T_2). The white arrow points to a baitDNA-bound hTopoIB on the DNA origami (highlighted with a white square). (D) AFM image of origamis as the ones depicted in (C) after incubation with hTopoIB−DNA cleavage complexes (the second step in the investigation of interaction mode T_2). The white arrow indicates a TopoIB−DNA cleavage complex interacting to an baitDNA-bound hTopoIB on the origami (highlighted with a white square). (E) and (F) AFM cross-section analysis of the naked and hTopoIB-bound part of an origami. (E) An AFM image with cross-sections through the naked part of the origami (red line) and through the hTopoIB-bound part of the origami (black line). (F) A graphical representation of the cross-section analysis. (G) Histogram showing the quantification of the binding efficiency between hTopoIB cleavage complexes and bait DNA, *i.e.*, interaction mode T_1 (dark blue column) between free hTopoIB and baitDNA (medium blue column) and between hTopoIB cleavage complexes and baitDNA-bound hTopoIB, *i.e.*, interaction mode T_2 (light blue column).

Next, to investigate the T_2 interaction mode, excess purified hTopoIB−DNA cleavage complexes were incubated with the prepared DNA origami containing hTopoIB-bound baitDNA (as outlined in Figure 3C and D). Following several washing steps, as described above, the resulting DNA origamis were subjected to AFM imaging. As demonstrated in Figure 4D, the AFM images revealed the occurrence of bright protrusions on the origami surfaces (an example is indicated by an arrow). The height of these protrusions was determined to be approximately 1.5 nm, corresponding to the expected AFM height of a single hTopoIB. However, the average width of some of the protrusions in Figure 4D was twice the size (34.2 ± 3.7 nm) of the width (15.6 ±

3.5 nm) of hTopoIB−DNA cleavage complexes bound to naked baitDNA, as calculated by line profile measurements (see Supporting Information, Figure S3), and these protrusions are therefore likely to represent binding between a hTopoIB−DNA cleavage complex and a hTopoIB−baitDNA complex anchored on the DNA origami surfaces, *i.e.*, the T_2 interaction mode.

Compared to the T_1 interaction mode and the binding of free hTopoIB to the baitDNA both giving rise to binding complexes on ~30% of the entire population of origami binding sites, the T_2 interaction mode appeared rather ineffective with only 10.3 ± 6% of DNA origamis exposing a hTopoIB-bound baitDNA being bound by a TopoIB−DNA cleavage complex, as determined by counting 88 origamis with a hTopoIB-occupied baitDNA. Hence, the binding frequency of the T_2 interaction mode was a least three-fold lower than the binding frequency of the T_1 interaction mode, which on the other hand corresponded to the binding frequency of free hTopoIB to baitDNA.

These results strongly support that the existence of a secondary binding site in hTopoIB can account for the filament formation and the intra- or intermolecular nodes observed upon incubation of the enzyme with relaxed circular DNA (Figure 2). Although we did observe some interaction of the T_2 mode (interaction between two hTopoIB−DNA complexes), the frequency of these interactions was quite low and may be anticipated to be of less importance for filament and node formation. The relatively low number of T_2 interactions may be the result of two DNA-bound hTopoIB enzymes interacting directly with rather low efficiency either unspecifically or maybe via traces of traits inherited from a common ancestor shared with the tyrosine recombinases, which are well-known to form synapses via protein−protein interactions.[15,16]

Alternatively, the T_2 interactions may be the result of a hTopoIB in complex with one DNA fragment interacting with the DNA moiety of another hTopoIB−DNA complex. The baitDNA and DNA cleavage substrate used for the current study were composed of 21 and 32 base pairs of double-stranded DNA, respectively, as well as a stretch of single-stranded DNA to promote the anchoring of the baitDNA in the origami or the purification of cleavage complexes (see Supporting Information, Figures S1 and S2, respectively). These DNA fragments were chosen so that they would support binding or cleavage by hTopoIB and still ensure close to full coverage of the entire DNA helix of each fragment by a single hTopoIB. Here it is important to point out that binding by hTopoIB protects ~20−25 base pairs in traditional footprinting assays.[30,31] Hence, the length (21 base pairs) of the baitDNA represents the very minimal stretch of double-stranded DNA anticipated to support DNA binding and is expected to be fully covered by hTopoIB upon binding. However, the DNA cleavage substrate of 32 base pairs, which was found to be the minimal length supporting cleavage sufficiently effective to allow for preparation of the necessary amounts of purified cleavage complexes (data not shown), may lead to the exposure of 4−8 base pairs of naked DNA after hTopoIB binding. DNA interaction by the secondary binding site in draTopoIB involves 4−5 base pairs.[14] It is, therefore, possible that the observed T_2 interactions are *de facto* the result of interactions between the secondary binding site in a DNA-bound hTopoIB and a double-stranded DNA moiety of a second hTopoIB−DNA complex that is exposed, as described above, and/or by a certain degree of breathing within a hTopoIB−DNA complex. At present we cannot rule out a putative interaction between the secondary binding site in baitDNA-bound hTopoIB and the single-stranded part of the cleavage complexes, which was used for purification.

In all AFM images, the DNA-free hTopoIB or cleavage complexes bound to the DNA origami occupy different positions. This is mainly due to the length of the DNA moieties and the flexibility of the double-stranded baitDNA protruding from the DNA origami surfaces. Moreover, the relatively weak interaction can be easily manipulated by the AFM tip during scanning (see further explanation in Supporting Information, Figures S4−6).

CONCLUSION

In the present study we use atomic force microscopy (AFM) imaging to demonstrate that human topoisomerase I (hTopoIB) when incubated with relaxed circular DNA, forms inter- and intramolecular synapses, in which distinct DNA segments are brought together at protein-containing nodes or within filamentous protein stems. We use a two-dimensional (2D) DNA origami template with a protruding baitDNA fragment at an addressable position in combination with AFM imaging to investigate the molecular mechanism behind the observed synapsis formation at the single molecule level. The presented results are to our knowledge the first demonstration of the direct and simultaneous interaction of hTopoIB to two distinct DNA helices, which strongly supports the existence of a secondary DNA binding site in this enzyme. Such a site may provide DNA crossover recognition potential to the enzyme which in turn may function as a "topological sensor" directing hTopoIB action to plectonemic supercoiled DNA.

METHODS

Enzymes and Reagents. All DNA oligonucleotides were purchased from DNA Technology A/S. All oligonucleotides were high-performance liquid chromatography (HPLC) purified and ethanol precipitated. M13mp18 viral DNA, oligo(dT)25 cellulose, and T4 polynucleotide kinase were purchased from New England Biolabs. Microcon centrifugal filter YM-100 devices (100 000 molecular weight cutoff, MWCO) were purchased from Millipore, and Mobicols columns were from MoBiTec.

Enzyme Preparation. Recombinant hTopoIB was expressed in yeast and purified to homogeneity, as described previously.[28] The enzyme preparation was tested for purity by sodium dodecyl sulfate (SDS) polyacrylamide gel electrophoresis followed by Coomassie staining before subjection to AFM experiments.

Circular DNA Preparation. Circular pUC19 plasmid DNA was prepared from *E. coli* using the standard miniprep kit from Qiagen, essentially as described by the manufacturer. To relax supercoils in the plasmid, it was incubated with 10 times molar excess of hTopoIB in a buffer containing 150 mM NaCl, 10 mM Tris−HCl pH 7.5, 5 mM $MgCl_2$, and 5 mM $CaCl_2$ for 30 min at 37 °C. The plasmid was run on a 1% agarose gel, and the fully relaxed plasmid was cut out of the gel before the plasmid was extracted using the standard gel extraction kit from Qiagen. The plasmid concentration was estimated, and the purity confirmed by spectrophotometric measurement.

AFM Imaging and Analysis of hTopoIB. For AFM imaging of hTopoIB, 0.05 pmol of purified hTopoIB was deposited on the freshly cleaved mica surface (Ted Pella, Inc.) and left to adsorb for 2−3 min. Then 70 μL of TAEM/Mg^{2+} (40 mM Tris-HCl pH 8.0, 2mM EDTA, and 10 or 12.5 mM MgAc (as stated in text)) buffer (10 mM of Mg^{2+}) was added and left for 30 min and measured by AFM under liquid condition. The obtained images were flattened followed by automated analysis using the Scanning Probe Image Processor (SPIP) software (Image Metrology ApS, version 5.2, Lyngby, Denmark) to yield size histograms of the imaged particles. The Gauss fitting was performed by using the equation:

$$y = y_0 + \left\{ \frac{A}{(w \times \sqrt{(\mathrm{PI}/2)})} \right\} \exp^{(-2((x\ -\ xc)/w)^2)}$$

to calculate the average height and width.

AFM Imaging of hTopoIB—Plasmid DNA Complexes. 0.2 pmol of hTopoIB was mixed with 0.05 pmol of relaxed circular DNA and incubated for 5 min at room temperature. The samples were deposited onto a freshly cleaved mica surface (Ted Pella, Inc.), left to adsorb for 5 min, then rinsed with distilled water, and dried under a gentle stream of nitrogen before AFM imaging under dry condition.

hTopoIB—DNA Cleavage Complexes Preparation and Purification. For generation of the hTopoIB−DNA cleavage complexes, 100 pmol of a synthetic suicide cleavage substrate composed of a top cleavage strand (5′-GAT CTG CAA GAC TTA G-3′), which is cleaved by hTopoIB, a top noncleavage strand (5-AGA AAA ATT TTT CCG CTG-3′), and a bottom strand (5′-CAG CGG AAA AAT TTT TCT AAG TCT TGC AGA TCA AAA AAA AAA AA-3′) was used. The top noncleavage strand was 5′-phoshorylated by T4 polynucleotide kinase (to prevent ligation by hTopoIB), and the substrate hybridized as previously described.[32] Subsequently, the substrate was passed 5 times over a 50 μL column of oligo(dT)25 cellulose in a buffer containing 10 mM Tris−HCl pH 7.5, 5 mM $MgCl_2$, and 5 mM $CaCl_2$ at 4 °C to facilitate binding of the substrate to the column matrix. Covalent hTopoIB−DNA cleavage complexes were generated by 5 times recycling of a solution containing 10 mM Tris−HCl pH 7.5, 5 mM $MgCl_2$, 5 mM $CaCl_2$, and a 10-fold molar excess of recombinant hTopoIB over the column at 4 °C. The column was washed in 1 M NaCl, 10 mM Tris−HCl pH 7.5, and 1 mM EDTA at 4 °C to remove unreacted hTopoIB. Subsequently, hTopoIB−DNA cleavage complexes were eluted dropwise in a buffer containing 10 mM Tris−HCl pH 7.5 and 1 mM EDTA by raising the temperature to 37 °C, which melts the annealing between the polyA stretch of the cleavage substrate and the oligo(dT)25 cellulose matrix. The resulting fractions were analyzed by SDS polyacrylamide gel electrophoresis, and the generated hTopoIB−DNA cleavage complexes visualized by Coomassie staining (S2). Morever, the eluted fractions were tested for catalytic activity and found inert in a standard relaxation assay[33] (data not shown).

Preparation and Imaging of DNA Origami. The rectangular DNA origami was modified at a predefined position to extend the baitDNA composed of the oligonucleotides: 5′-ATG CTT GTC AGT CAG TAA CCG TAC TGC GGT ATT ATA GTC AGA AGC CTC CAA CAG GTC AGG ATT TAA ATA and 5′-CGG TTA CTG ACT GAC AAG CAT (see Supporting Information, Figure S1). A mixture containing the viral DNA and all the staple strands (including the baitDNA oligonucleotides) at a molar ratio of 1:20 was heated to 90 °C and slowly cooled to 4 °C to allow self-assembly of the DNA origami by annealing.[19] The fully assembled DNA origami entities were purified using Microcon centrifugal filter devices (100 000 MWCO, 300 × g speed, 10 min.) followed by washing with TAEM/Mg^{2+} (12.5 mM Mg^{2+}) buffer to get rid of the excess free staple strands. Purified origami was deposited onto a freshly cleaved mica surface, left to adsorb for 5 min and then imaged with TAEM/Mg^{2+} (12.5 mM Mg^{2+}) buffer in liquid environments. The hTopoIB or hTopoIB−DNA complexes on the origami were also imaged in TAEM/Mg^{2+} (12.5 mM Mg^{2+}) buffer.

Assembly of hTopoIB—DNA Cleavage Complexes on DNA Origami. For generation of hTopoIB−DNA cleavage complexes on the DNA origami, 0.4 pmol of hTopoIB (in 10 mM Tris−HCl pH 7.5, 5 mM $MgCl_2$, 5 mM $CaCl_2$, and 1% glycerol) was added to the DNA origami and incubated for 30 min at room temperature. Subsequently unbound hTopoIB was removed by washing with a buffer containing 10 mM Tris−HCl pH 7.5, 5 mM $MgCl_2$, 5 mM $CaCl_2$, 1% glycerol, and 500 mM NaCl. Finally the mica surface was washed three times with slightly warm TAEM/Mg^{2+} (12.5 mM Mg^{2+}) buffer.

Atomic Force Microscope. AFM studies were carried out using the Agilent AFM 5500 (Agilent Technologies, USA) and the MultiMode SPM with a Nanoscope V controller (Veeco Instruments, Santa Barbara, CA) in both cases and operated in tapping-mode (TM-AFM). AFM cantilevers used liquid conditions and had a typical resonance frequency $\upsilon_0 \approx 7$ kHz and a spring constant of 0.4 N m^{-1} (Olympus cantilevers, OMLC-400TRP-2). For the AFM tapping studies in air, LTESP cantilevers were used (48 N m^{-1} force constant). Typically the scan frequencies were 1−2 Hz with minimal loading forces applied and optimized feedback parameters. All the recorded AFM images consist of 512 × 512 pixels, and several AFM images were obtained at separate locations across the mica surfaces to ensure a high degree of reproducibility of the recorded molecular nanostructures. The AFM images were analyzed by using the commercial Scanning Probe Image Processor (SPIP) software (Image Metrology ApS, version 5.2, Lyngby, Denmark).

Acknowledgment. The authors acknowledge financial support from the Danish National Research Foundation and the Danish Ministry for Science, Technology, and Innovation through the iNANO Center and from the Danish Research Councils, the Danish Cancer Society, the Novo Nordisk Foundation, the Carlsberg Foundation, the Augustinus Foundation, Civilingeniør Frode V. Nyegaard og hustru's Foundation, Direktør Einar Hansen og hustru fru Vera Hansen's Foundation, Fabrikant Einar Willumsen's Mindelegat, the Harboe Foundation, Karen Elise Jensen's Foundation, Købmand Sven Hansen og hustru Ina Hansen's Fondation, Aage og Johanne Louis-Hansens Foundation, the Hørslev Foundation, and the Foundation til Lægevidenskabens fremme.

Supporting Information Available: Schematic representation of the DNA origami design and preparation of purified hTopoIB−DNA cleavage complexes, line profile measurements discriminating between T_1 and T_2 interaction modes, and large scale images of hTopoIB or hTopoIB−DNA cleavage complexes bound to the DNA origami. This material is available free of charge *via* the Internet at http://pubs.acs.org.

REFERENCES AND NOTES

1. Champoux, J. J. DNA Topoisomerases: Structure, Function, and Mechanism. *Annu. Rev. Biochem.* **2001**, *70*, 369–413.
2. Jaxel, C.; Kohn, K. W.; Pommier, Y. Topoisomerase I Interaction with SV40 DNA in the Presence and Absence of Camptothecin. *Nucleic Acids Res.* **1988**, *16*, 11157–11170.
3. Shen, C. C.; Shen, C. K. Specificity and Flexibility of the Recognition of DNA Helical Structure by Eukaryotic Topoisomerase I. *J. Mol. Biol.* **1990**, *212*, 67–78.
4. Parker, L. H.; Champoux, J. J. Analysis of the Biased Distribution of Topoisomerase I Break Sites on Replicating Simian Virus 40 DNA. *J. Mol. Biol.* **1993**, *231*, 6–18.

5. Madden, K. R.; Stewart, L.; Champoux, J. J. Preferential Binding of Human Topoisomerase I to Superhelical DNA. *EMBO J.* **1995**, *14*, 5399–5409.
6. Müller, M. T. Quantitation of Eukaryotic Topoisomerase I Reactivity with DNA. Preferential Cleavage of Supercoiled DNA. *Biochim. Biophys. Acta* **1985**, *824*, 263–267.
7. Camilloni, G.; Martino, E. D.; Caserta, M.; Mauro, E. D. Eukaryotic DNA Topoisomerase I Reaction is Topology Dependent. *Nucleic Acids Res.* **1988**, *16*, 7071–7085.
8. Caserta, M.; Amadei, A.; Camilloni, G.; Mauro, E. D. Regulation of the Function of Eukaryotic DNA Topoisomerase I: Analysis of the Binding Step and of the Catalytic Constants of Topoisomerization as a Function of DNA Topology. *Biochemistry* **1990**, *29*, 8152–8157.
9. Zechiedrich, E. L.; Osheroff, N. Eukaryotic Topoisomerases Recognize Nucleic Acid Topology by Preferentially Interacting with DNA Crossovers. *EMBO J.* **1990**, *9*, 4555–4562.
10. Yang, Z.; Carey, J. F.; Champoux, J. J. Mutational Analysis of the Preferential Binding of Human Topoisomerase I to Supercoiled DNA. *FEBS J.* **2009**, *276*, 5906–5919.
11. Staker, B. L.; Hjerrild, K.; Feese, M. D.; Behnke, C. A.; Burgin, A. B., Jr.; Stewart, L. The Mechanism of Topoisomerase I Poisoning by a Camptothecin Analog. *Proc Natl Acad Sci U.S.A.* **2002**, *99*, 15387–15392.
12. Shuman, S.; Bear, D. G.; Sekiguchi, J. Intramolecular Synapsis of Duplex DNA by Vaccinia Topoisomerase. *EMBO J.* **1997**, *3*, 6584–6589.
13. Moreno-Herrero, F.; Holtzer, L.; Koster, D. A.; Shuman, S.; Dekker, C.; Dekker, N. H. Atomic Force Microscopy Shows that Vaccinia Topoisomerase IB Generates Filaments on DNA in a Cooperative Fashion. *Nucleic Acids Res.* **2005**, *33*, 5945–5953.
14. Patel, A.; Yakovleva, L.; Shuman, S.; Mondragón, A. Crystal Structure of a Bacterial Topoisomerase IB in Complex with DNA Reveals a Secondary DNA Binding Site. *Structure* **2010**, *18*, 725–733.
15. Shuman, S. Vaccinia Virus DNA Topoisomerase: a Model Eukaryotic Type IB Enzyme. *Biochim. Biophys. Acta* **1998**, *1400*, 321–337.
16. Grainge, I.; Jayaram, M. The Integrase Family of Recombinase: Organization and Function of the Active Site. *Mol. Microbiol.* **1999**, *33*, 449–456.
17. Chen, Y.; Narendra, U.; Iype, L. E.; Cox, M. M.; Rice, P. A. Crystal Structure of a Flp Recombinase-Holliday Junction Complex: Assembly of an Active Oligomer by Helix Swapping. *Mol. Cell* **2000**, *6*, 885–897.
18. Guo, F.; Gopaul, D. N.; van Duyne, G. D. Structure of Cre Recombinase Complexed with DNA in a Site-Specific Recombination Synapse. *Nature* **1997**, *389*, 40–46.
19. Rothemund, P. W. K. Folding DNA to Create Nanoscale Shapes and Patterns. *Nature* **2006**, *440*, 297–302.
20. Maune, H. T.; Han, S. P.; Barish., R. D.; Bockrath, M.; Lii, W. A. G.; Rothemund, P. W. K.; Winfree, E. Self-assembly of Carbon Nanotubes into Two-Dimensional Geometries Using DNA Origami Templates. *Nat. Nanotechnol.* **2010**, *5*, 61–66.
21. Sharma, J.; Chhabra, R.; Andersen, C. S.; Gothelf, K. V.; Yan, H.; Liu, Y. Toward Reliable Gold Nanoparticle Patterning on Self-assembled DNA Nanoscaffold. *J. Am. Chem. Soc.* **2008**, *130*, 7820–7821.
22. Hung, A.; Micheel, C. M.; Bozano, L. D.; Osterbur, L. W.; Wallraff, G. M.; Cha, J. N. Large-Area Spatially Ordered Arrays of Gold Nanoparticles Directed by Lithographically Confined DNA Origami. *Nat. Nanotechnol.* **2009**, *5*, 121–126.
23. Kuzyk, A.; Laitinen, K. T.; Törmä, P. DNA Origami as a Nanoscale Template for Protein Assembly. *Nanotechnology* **2009**, *20*, 235305.
24. Kuzuya, A.; Kimura, M.; Numajiri, K.; Koshi, N.; Ohnishi, T.; Okada, F.; Komiyama, M. Precisely Programmed and Robust 2D Streptavidin Nanoarrays by Using Periodical Nanometer-Scale Wells Embedded in DNA Origami Assembly. *ChemBioChem* **2009**, *10*, 1811–1815.
25. Stephanopoulos, N.; Liu, M.; Tong, G. J.; Li, Z.; Liu, Y.; Yan, H.; Francis, M. B. Immobilization and One-Dimensional Arrangement of Virus Capsids with Nanoscale Precision Using DNA Origami. *Nano Lett.* **2010**, *10*, 2714–2720.
26. Endo, M.; Katsuda, Y.; Hidaka, K.; Sugiyama, H. Regulation of DNA Methylation Using Different Tensions of Double Strands Constructed in a Defined DNA Nanostructure. *J. Am. Chem. Soc.* **2010**, *132*, 1592–1597.
27. Voigt, N. V.; Torring, T.; Rotaru, A.; Jacobsen, M. F.; Ravnsbaek, J. B.; Subramani, R.; Mamdouh, W.; Kjems, J.; Mokhir, A.; Besenbacher, F.; et al. Single-Molecule Chemical Reactions on DNA Origami. *Nat. Nanotechnol.* **2010**, *5*, 200–203.
28. Lisby, M.; Krogh, B. O.; Boege, F.; Westergaard, O.; Knudsen, B. R. Camptothecins Inhibit the Utilization of Hydrogen Peroxide in the Ligation Step of Topoisomerase I Catalysis. *Biochemistry* **1998**, *37*, 10815–10827.
29. Redinbo, M. R.; Stewart, L.; Kuhn, P.; Champoux, J. J.; Hol, W. G. Crystal Structures of Human Topoisomerase I in Covalent and Noncovalent Complexes with DNA. *Science* **1998**, *279*, 1504–1513.
30. Stevnsner, T.; Mortensen, U. H.; Westergaard, O.; Bonven, B. J. Interactions Between Eukaryotic DNA Topoisomerase I and a Specific Binding Sequence. *J. Biol. Chem.* **1989**, *264*, 10110–10113.
31. Bendixen, C.; Thomsen, B.; Alsner, J.; Westergaard, O. Camptothecin-stabilized Topoisomerase I-DNA Adducts Cause Premature Termination of Transcription. *Biochemistry* **1990**, *29*, 5613–5619.
32. Andersen, F. F.; Andersen, K. E.; Kusk, M.; Frøhlich, R. F.; Westergaard, O.; Andersen, A. H.; Knudsen, B. R. Recombinogenic Flap Ligation Mediated by Human Topoisomerase I. *J. Mol. Biol.* **2003**, *330*, 235–246.
33. Lisby, M.; Olesen, J. R.; Skouboe, C.; Krogh, B. O.; Straub, T.; Boege, F.; Velmurugan, S.; Martensen, P. M.; Andersen, A. H.; Jayaram, M.; et al. Residues Within the N-terminal Domain of Human Topoisomerase I Play a Direct Role in Relaxation. *J. Biol. Chem.* **2001**, *276*, 20220–20227.